Pergamon

PII: S1359-6454(97)00204-8

*Acta mater.* Vol. 46, No. 2, pp. 651–666, 1998
Acta Metallurgica Inc.
Published by Elsevier Science Ltd
Printed in Great Britain
1359-6454/98 $19.00 + 0.00

# REACTIVE DIFFUSION AND PHASE EQUILIBRIA IN THE V–C, Nb–C, Ta–C AND Ta–N SYSTEMS

**H. WIESENBERGER, W. LENGAUER† and P. ETTMAYER**

Institute for Chemical Technology of Inorganic Materials, Vienna University of Technology, Getreidemarkt 9/161, A-1060 Vienna, Austria

*(Received 5 February 1997; accepted 11 June 1997)*

**Abstract**—The reactive formation of vanadium, niobium and tantalum carbides as well as tantalum nitrides was investigated by means of diffusion couples. For the preparation of the carbides the compact metals were reacted with graphite powder and the formation of the phases $MeC_{1-x}$ and $Me_2C$ could be observed. The slow growth rate of the $Me_4C_3$ phases made it necessary to provide restricted diffusion geometry (wedge-type or plane-sheet samples) or, preferentially, diffusion couples of the type $Me_2C$/graphite. The phases $\zeta$-$V_4C_{3-x}$, $\zeta$-$Nb_4C_{3-x}$ and $\zeta$-$Ta_4C_{3-x}$ could be observed as distinct diffusion bands below 1900, 1575 and 2170°C, respectively. The compositions of the phase boundaries as a function of temperature were measured by EPMA. The composition of $\zeta$-$V_4C_{3-x}$ is 37.9 at.%C (with a narrow homogeneity range of $<0.5$ at.%C), that of $\zeta$-$Nb_4C_{3-x}$ is 40.1–40.7 at.%C and that of $\zeta$-$Ta_4C_{3-x}$ is 38.2–39.0 at.%C (standard deviations *ca.* $\pm 0.2$ at.%C). For the $\beta$-$Me_2C$ phases the carbon content was found to be greater than the values given in recent assessments, whereas the homogeneity regions measured for the $\delta$-$MeC_{1-x}$ phases are consistent with established data. In the Ta–N system the $\varepsilon$-TaN and the $\delta$-$TaN_{1-x}$ phases usually form very narrow phase bands. Here again wedge-type diffusion samples were applied in order to enlarge the thickness of the phase bands. $\delta$-$TaN_{1-x}$ undergoes a eutectoid decomposition at $1821 \pm 19$°C into $\varepsilon$-TaN and $\beta$-$Ta_2N$. The formation of $\varepsilon$-TaN occurs at $1888 \pm 15$°C at 25 bar $N_2$, its homogeneity range at 1873°C is smaller than 0.4 at.%N. Re-investigated portions of the phase diagrams of all four systems are given.

## 1. INTRODUCTION

The VB transition metal–carbon systems have been extensively investigated. The system V–C was critically reviewed by Carlson *et al.* [1] in 1989 and by Huang [2] in 1991, the Nb–C system by Smith *et al.* [3] in 1986. The Ta–C system was recently thermochemically modelled by Frisk and Fernández Guillermet [4]. The phase diagrams generally appear to be well established but there are still open questions such as the location of some phase boundaries (i.e. the carbon-poor and carbon-rich phase boundaries of the $\beta$-$Me_2C$ phases).

The greatest deficiency of knowledge exists for the phases $\zeta$-$V_4C_{3-x}$, $\zeta$-$Nb_4C_{3-x}$ and $\zeta$-$Ta_4C_{3-x}$. Storms and McNeal [5] reported the existence of the $\zeta$-$V_4C_{3-x}$ phase and gave a peritectoid decomposition temperature of 1344°C. Later, other investigators observed this phase above a temperature of 1500°C [6, 7]. Khaenko and Fak [8] estimated a decomposition temperature between 1250 and 1600°C. Ghaneya and Carlson [9] gave 1320°C, with a composition of 39.7 at.%C. Storms and McNeal [5] and Ghaneya and Carlson [9] explained the fact that $\zeta$-$V_4C_{3-x}$ had been observed in samples annealed at temperatures higher than 1344 and 1320°C, respectively, with its formation during the cooling period.

While the existence of $\zeta$-$V_4C_{3-x}$ is well accepted, there are doubts about the existence of $\zeta$-$Nb_4C_{3-x}$ as pointed out in the work of Smith *et al.* [3]. In bulk samples Brauer and Lesser [10] observed some weak X-ray reflections, which they attributed to $\zeta$-$Nb_4C_{3-x}$ but they were unable to increase the amount of this phase by heat treatment. Storms and Krikorian [11] and Elliot [12] could not find any indication of the existence of this phase. Rudy *et al.* [7] detected weak X-ray reflections of the $\zeta$ phase in bulk samples at 1800°C, but they could not observe it by means of diffusion experiments at 1600°C.

In the Ta–C system the phase equilibria between the phases $\beta$-$Ta_2C$ and $\delta$-$TaC_{1-x}$ are well established [14], but there are uncertainties about the exact homogeneity range and decomposition temperature of the compound $\zeta$-$Ta_4C_{3-x}$ [15]. Initial evidence for the existence of a $\zeta$ phase was reported by Lesser and Brauer [16]. In bulk samples they observed extra X-ray reflections, which they attributed to $\zeta$-$Ta_4C_{3-x}$. Later, Zaplatynsky [17] observed $\zeta$-$Ta_4C_{3-x}$ precipitations in diffusion samples prepared at 2500°C, whereas Brizes and Tobin [18] could observe a distinct $\zeta$-$Ta_4C_{3-x}$ diffusion layer. The latter authors reported a decomposition temperature in the range 2150–2250°C

†To whom all correspondence should be addressed.

and a composition of 41.7 at.%C by means of EPMA, which is very close to the ideal composition implied by a crystallochemical model [13]. Recently, a thermodynamic modeling of the Ta–C system was performed by Frisk and Fernández Guillermet [4] but $\zeta$-$Ta_4C_{3-x}$ was not included in the treatment due to a lack of data.

The structure of the $\zeta$ phases was investigated by Yvon and Parthé [13] with a single crystal of $\zeta$-$V_4C_{3-x}$ (the sample contained also some $\beta$-$V_2C$). Lattice parameters were also given for $\zeta$-$Nb_4C_{3-x}$ and $\zeta$-$Ta_4C_{3-x}$. The latter phases were reported to be isostructural with $\zeta$-$V_4C_{3-x}$ but no details were reported of how they had been prepared.

Several high-temperature investigations were made in the Ta–N system. The solubility of nitrogen in tantalum was given by Fromm and coworkers [19, 20] as a function of temperature. It is much greater than the solubility of carbon in tantalum. For the tantalum-rich limit of the hexagonal phase $\beta$-$Ta_2N$, Gebhardt *et al.* [20] measured a composition of 23 at.%N at 2000°C. Booker and Brukl [21] reported a nitrogen content of 30 at.%N at this temperature. For the nitrogen-rich limit a composition of 33.3 at.%N was assumed [14, 20]. Gatterer *et al.* [22] established a eutectoid equilibrium of $\delta$-$TaN_{1-x} \rightarrow \varepsilon$-TaN + $\beta$-$Ta_2N$ with an invariant temperature of $1750 \pm 50$°C and a eutectoid composition of $\delta$-$TaN_{1-x}$ of 42 at.%N, corresponding to $\delta$-$TaN_{0.72}$. Above this temperature they could prepare the $\delta$-$TaN_{1-x}$ phase with a nitrogen pressure of more than 10 bar. The $\varepsilon$-TaN phase shows a very narrow homogeneity range [23] and decomposes at normal pressure above 1500°C, at a pressure of 4 bar $N_2$ above 1600°C and at 10 bar $N_2$ above 2000°C [24]. Politis and Rejman [25] found that $\delta$-$TaN_{1-x}$ (prepared from $\varepsilon$-TaN starting material) can be stabilized by small additions of carbon (0.2 wt%) so that the pressure/temperature data on the formation of $\delta$-$TaN_{1-x}$ are very sensitive to carbon impurities. They also prepared diffusion layers of tantalum nitrides including $Ta_5N_6$ by high-pressure annealing of Ta wires and proposed a Ta–N phase diagram based upon their own and literature data which shows a decomposition temperature of around 1750°C for $\varepsilon$-TaN (at more than 100 bar $N_2$). The eutectoid composition of $\delta$-$TaN_{1-x}$ was given to be near $TaN_{0.87}$ and was thus richer in nitrogen than that reported by Gatterer *et al.* [22]. The eutectoid temperature was given at 1600°C. The upper compositional limit of $\beta$-$Ta_2N$ was found to be [N]/[Ta] = 0.527 (at 1200 K) but a value of 0.50 was adopted for the phase diagram.

In view of these discrepancies encountered in the available data for all of the four systems a diffusion couple study was performed in order to clarify some of these points.

## 2. EXPERIMENTAL

### 2.1. Sample preparation

The starting material were V rods (99.9%; Heraeus, Germany), Nb metal rods and sheets (99.9%; Goodfellow, GB and Metallwerk Plansee, Austria), Ta sheet (>99.9 wt% Ta; Plansee, Austria), high-purity spectral graphite powder (VSPC, Ringsdorff, Germany) and high-purity nitrogen (>99.999 vol.% $N_2$, AGA, Austria).

The starting materials for $\beta$-$Me_2C$/C diffusion couples† were made by arc-melting pre-pressed mixtures of vanadium (>99.7 m% Nb; Goodfellow, GB) and niobium powder (>99.85 m% Nb; Goodfellow, GB) with VSPC graphite powder.

Sheets and wedges of vanadium, niobium and tantalum metals or of $Me_2C$ subcarbides with thicknesses of 1–3 mm were packed into high-purity graphite in either a graphite or a molybdenum crucible and annealed in a cold-wall autoclave at various temperatures under argon atmosphere. The autoclave was equipped with a tungsten heating tube. Vanadium and vanadium carbides were annealed at temperatures from 1100 to 1900°C for 4–400 h; niobium and niobium carbides from 1500 to 2100°C for 6–575 h and tantalum carbide diffusion couples at temperatures from 1700 to 2200°C for 7 and 424 h. To ensure a good contact between metal and graphite at temperatures below 1300°C the design of the autoclave was modified in such a way that the metal was compressed between two graphite plates during heat treatment. The temperature was measured by a Pt30%Rh/Pt6%Rh thermocouple, a disappearing-filament pyrometer or a two-color infrared pyrometer, which were calibrated against each other. The gas pressure was measured with piezoelectric gauges. The temperature and pressure data were recorded during the full duration of the annealing experiments. Variation in temperature was less than ±15°C. The samples were heated up to the annealing temperature within 2 or 3 min and cooled down to below 600°C within 2–3 min (depending on the annealing temperature).

For the preparation of the Ta/$N_2$ diffusion couples, sheets and wedges of tantalum metal were placed in a crucible made from zirconium foil which served as a getter for the gas atmosphere. The samples were annealed in a cold-wall autoclave with a tungsten heating tube under nitrogen atmosphere. The temperature was measured through a silica window by a two-color infrared pyrometer and the gas pressure with piezoelectric gauges. Annealing experiments were performed at temperatures from 1400 to 2000°C for 20–500 h at three different pressures (1, 10 and 25 bar $N_2$). Pressure fluctuations remained below ±0.15 bar.

†The designation of diffusion couples refers to the starting materials, if the diffusion couples are named after the end members after the diffusion process the designation would be Me/$\delta$-MeC or $\beta$-$Me_2C$/$\delta$-MeC, respectively.

### 2.2. Metallography and XRD

After reaction the samples were cut with a diamond saw parallel to the diffusion direction, embedded into cold-setting resin and ground with 125 and 20 $\mu$m diamond discs. After ultrasonic cleaning the samples were polished with 3 $\mu$m diamond paste. The disc was cleaned every 30–45 min and new paste was applied. Finally the samples were polished with an aqueous suspension of $SiO_2$. The combined chemical and mechanical attack of the suspension improves the phase identification in polarized light. To obtain a good light-optical contrast the phases of the Nb/C, Ta/C and Ta/N diffusion couples were colored by anodical oxidation, the V/C diffusion couples were contrasted by interference films by reactive sputtering with iron oxide.

For phase identification the samples were examined by means of X-ray diffraction in Bragg–Brentano geometry with Cu-K$\alpha$ radiation (secondary monochromatized) and by use of a rotating sample holder to avoid texture effects in the $x$–$y$ plane and to offset the effects of the rather coarse-grained microstructure. In order to check the sequence of diffusion layers the samples were mounted on a steel cylinder and material was removed stepwise parallel to the surface by grinding with a diamond disk. X-ray diffractograms were taken after removal of every 5–10 $\mu$m to obtain information about the phase-bond sequence as a function of the depth.

### 2.3. EPMA-measurements

Microprobe analysis was performed with a Cameca Camebax SX50 microprobe equipped with five crystal spectrometers in a step scan mode with a step width from 3 to 10 $\mu$m in the direction of carbon diffusion. A W/Si multilayer crystal (60 Å lattice spacing) was used for the measurement of the carbon K$\alpha$ line, a LIF crystal for the V-K$\alpha$ line, a PET crystal for the Nb-L$\alpha$ line and a TAP crystal for the Ta-M$\alpha$ line intensities.

The measurements on vanadium carbide diffusion couples were performed with a counting time of 15 s per step, a beam of 100 nA and an accelerating voltage of 10 kV; for niobium carbide couples a counting time of 30 s per step for carbon and 10 s for niobium and a beam current of 300 nA and an accelerating voltage of 8 kV was chosen. The measurements in the Ta–C system were performed at 6 s per step for Ta and 30 s for C, with a beam current of 300 nA and an accelerating voltage of 6 kV. The data for the Ta–N samples were collected with 10 s for tantalum and 30 s per step for nitrogen, with a beam current of 300 nA and an accelerating voltage of 10 kV. The counting time was chosen in order to attain a confidence level for the measurements of the carbide phases of about 95%. The measurements of the carbon solubilities in V, Nb and Ta metal were disregarded because the sampling periods necessary to arrive at a statistically reliable counting rate were too long. On the other hand, measurements of the nitrogen content in Ta(N) yielded good results, the peak-to-background ratio of nitrogen being much higher than that of carbon. In addition, the solubility of N in Ta is much higher than the solubility of C in Ta.

Homotypic standardization was applied [26] (standard and investigated sample contain the same components) which ensures that influences from chemical bonding and the background function of sample and standard are similar. For the preparation of the standards thin metal plates (100–200 $\mu$m) were carburized by applying high temperatures and long diffusion times. The carbon content was determined by both, chemical analysis by Dumas gas chromatography, and weight gain. Both data sets were in excellent agreement. A detailed study of microphobic analysis of carbide and nitride diffusion couples was performed recently and the reader is referred to this study [27] for further details.

## 3. RESULTS AND DISCUSSION

### 3.1. Phase stabilities

In all Me/C diffusion couples the formation of $\delta$-$MeC_{1-x}$ and $\beta$-$Me_2C$ phase bands could easily be observed. At first glance, it was not possible to observe the $\zeta$-$Me_4C_{3-x}$ phase between these two phases by light-optical means. In the Ta–N system the nitrogen-richest phase, $\varepsilon$-TaN, also formed a very narrow phase band. Therefore, wedge-type and thin plane-sheet samples were employed. This 'finite' diffusion geometry of such samples causes a faster growth of diffusion layers because the proportionality factor $k$ of the diffusion-controlled layer growth (for with the relationship $x = k^*\sqrt{t}$ holds, where $x$ is the layer thickness and $t$ is the diffusion time) does not remain constant. Rather it becomes greater the thinner the sample becomes and, consequently, thin diffusion bands can be enlarged [28, 29]. This is shown in Fig. 1 for a V/C diffusion couple† where the $\zeta$-$V_4C_{3-x}$ phase was easily observable at the $\beta$-$V_2C$ tip of the wedge (Fig. 1, top-right microstructure) whereas this phase is too thin to be observed where the width of the sample is large (Fig. 1, top-left microstructure). The $\beta$-$V_2C$ core on the right has reached carbon saturation, whereas at the left side of the microstructure there is still $\alpha$-V(C) in the core. Thus an enhancement of the $\zeta$ phase band thickness was also possible by the use of $\beta$-$Me_2C$/C (plane-sheet and wedge-type) diffusion couples as a starting material. With this arrangement it was possible to prepare observable and continuous $\zeta$-$Me_4C_{3-x}$ phase bands

†The microstructures of this work are accessible under: http://info.tuwien.ac.at/physmet/images.html

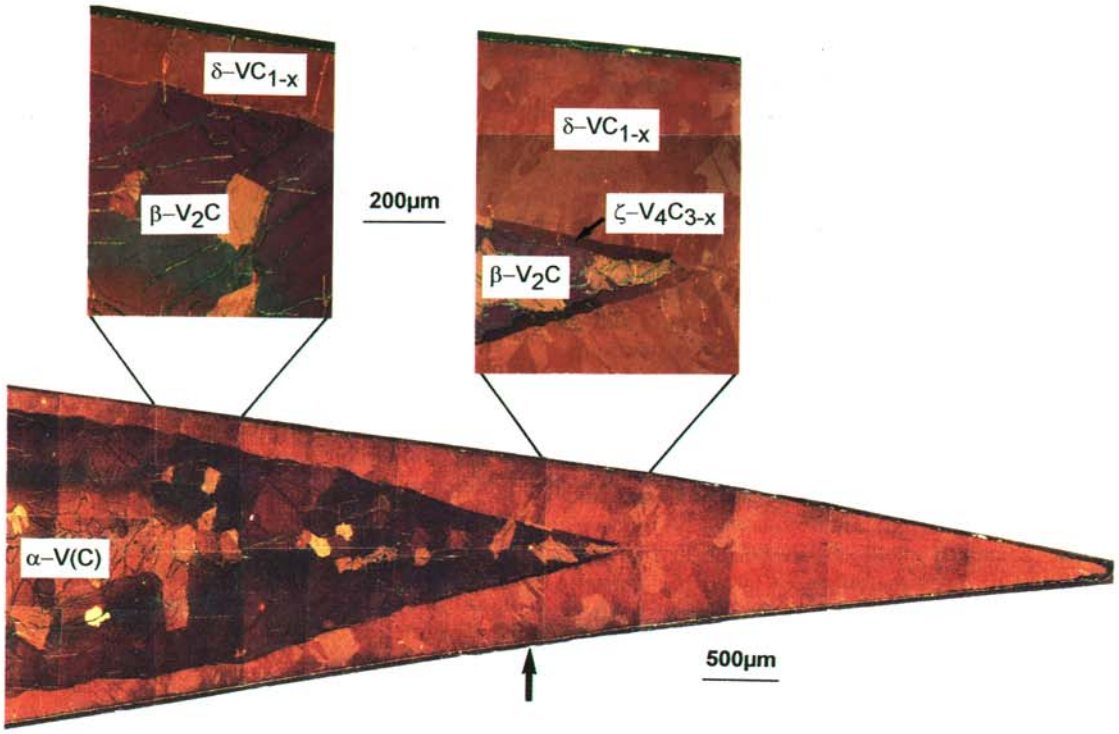


Fig. 1. Microstructure of a wedge-type V/C diffusion couple annealed at 1514°C for 48.0 h and quenched onto a copper plate. The $\zeta$-$V_4C_{3-x}$ phase is visible only at the tip of the wedge-shaped $\beta$-$V_2C$ phase where $\beta$-$V_2C$ is carbon saturated; it is not visible at positions where the sample is thick; i.e. where the carbon concentration gradient is steep. Contrasted with iron oxide, polarized light. The arrows at the bottom indicate the position of the EPMA scan [Fig. 9(a)].

within shorter diffusion times than with the Me/C diffusion couples.

These results also indicate that a conclusion of whether a phase, which forms a thin phase band, is absent because of thermal instability or is unobservable because of a too small band width, is impossible if diffusion couples with a quasi (semi-)infinite diffusion geometry are employed.

*3.1.1. The V–C system.* Because of the slow growth rate of $\zeta$-$V_4C_{3-x}$ and in order to find the appropriate diffusion times a series of $\beta$-$V_2C$/C diffusion couples were prepared at three different temperatures (Fig. 2). While at 1267°C a continuous $\zeta$-$V_4C_{3-x}$ phase band could be observed only after an annealing of 78 h, it formed readily at 1562°C after only 0.8 h. Figure 2 illustrates how long the samples have to be annealed in order to develop the observable $\zeta$-$V_4C_{3-x}$ phase bands. From the results reported in the literature, it can be suspected that in many instances the samples have not been annealed long enough to make this phase observable. In addition, many samples had been bulk samples where microstructural phase identification is less reliable and where XRD probably is not sensitive enough to detect small amounts of a phase.

The $\zeta$-$V_4C_{3-x}$ phase was detected in all samples quenched from temperatures up to 1710°C. This does not correspond to data given by Ghaneya and Carlson [9], who measured a decomposition temperature of 1320°C by DTA. They also found $\zeta$-$V_4C_{3-x}$ in samples which they had annealed above 1320°C, but explained this apparent inconsistency assuming that the phase was formed during the cooling period. Since in the present investigation the formation of the $\zeta$ phase could be observed only after a minimum annealing period of 100 h at $T = 1280$°C and of 20 h at $T = 1400$°C, it appears to be rather unlikely that this phase should form within a short cooling period (compare with results of high-temperature experiments described below). Furthermore, DTA measurements are probably inadequate to detect slow phase reactions of solid–solid phase equilibria, particularly in view of the comparatively small energy changes (compare [30]). In addition, by DTA, the phases involved in the reaction cannot be identified (such as by metallograph and XRD) so that DTA peaks can be misinterpreted. The decomposition temperature of 1344°C given by Storms and McNeal [5] was derived rather indirectly from the change in the lattice parameter of $\delta$-$VC_{1-x}$ with the annealing

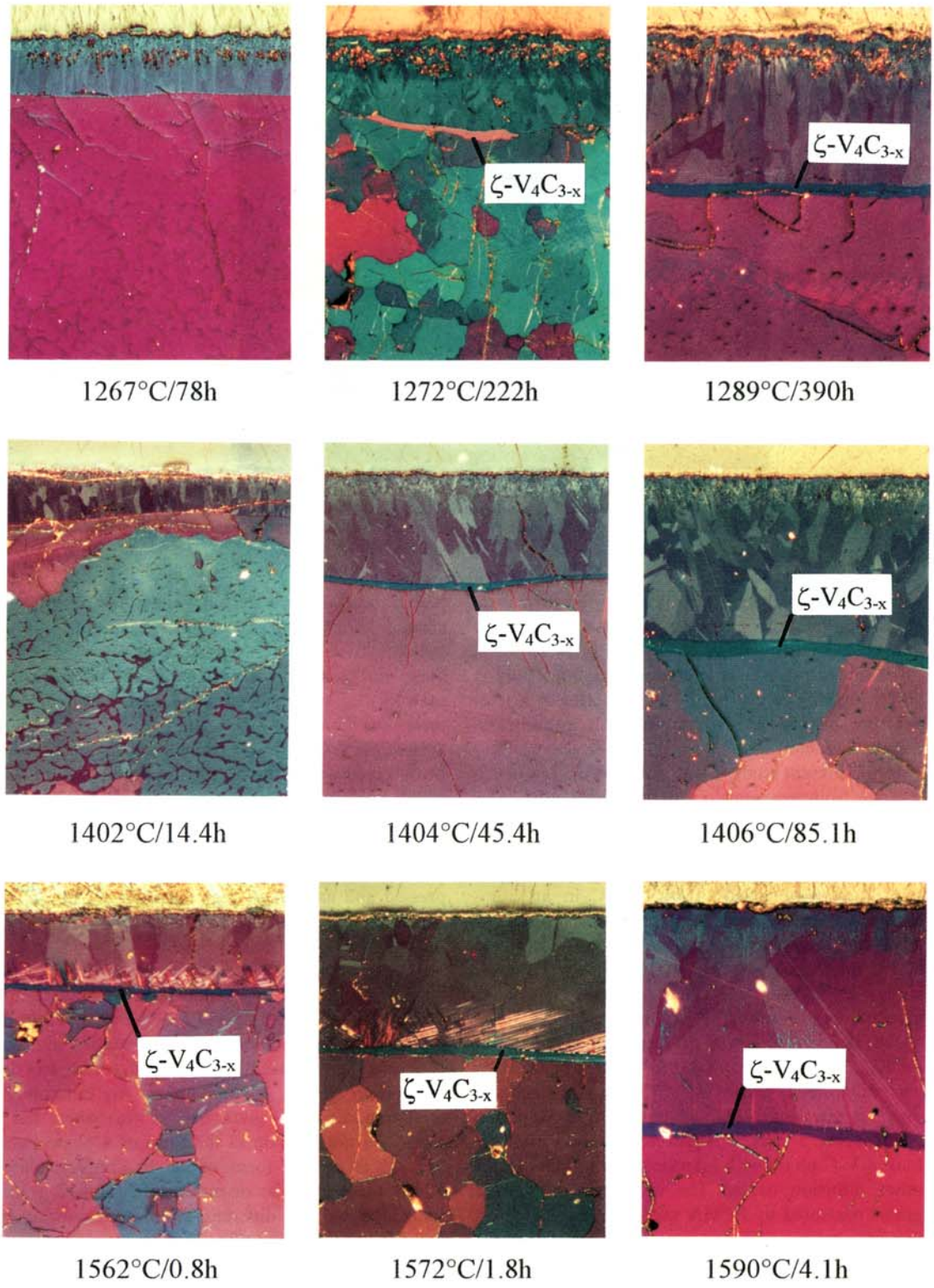


Fig. 2. Microstructures of $\beta$-$V_2C$/C diffusion couples annealed at three different temperature ranges for different times. The $\zeta$-$V_4C_{3-x}$ phase band forms relatively slowly between $\delta$-$VC_{1-x}$ (top) and $\beta$-$V_2C$ (bottom) and after an induction period. Contrasted with iron oxide, polarized light.


Fig. 3. Microstructure of a V/C diffusion couple annealed at 1496°C for 123.5 h, etched with an aqueous solution of $HNO_3$. Polarized light. The orange and blue colored areas are regions of formation of ordered vanadium carbide phases.

temperature which was attributed to the formation of the $\zeta$ phase. They, too, observed $\zeta$-$V_4C_{3-x}$ above 1344°C. In a later work by Storms *et al.* [6] this temperature was not referred to again. Rudy *et al.* [7] observed a distinct $\zeta$-$V_4C_{3-x}$ layer at a temperature of 1500°C in samples with a diffusion-couple character.

In the present study it was not possible to quench samples from temperatures higher than 1710°C. For annealing experiments at higher than 1710°C a $\zeta$-$V_4C_{3-x}$ phase band was prepared from $\beta$-$V_2C$/C couples annealed for 4 h at 1600°C. These couples were then re-annealed at $T \leqslant 1900$°C in an autoclave and without a graphite bed in order to achieve a higher cooling rate (cooling down to 800°C took about 30 s). $\beta$-$V_2C$/C diffusion couples with $\beta$-$V_2C$ containing 33 at.%C were found to give the best results (31, 32 and 33 at.%C were tested) concerning a well-developed non-interrupted $\zeta$-$V_4C_{3-x}$ phase band. At 1850°C the $\zeta$ phase band was still present but at 1900°C it was absent and only a few individual elongated $\zeta$ precipitates (thicknesses: 5–max.25 $\mu$m) were formed within the bulk $\beta$-$V_2C$ phase with interfaces not parallel to the other diffusion bands. The composition of these grains measured by EPMA was 37.2 at.%C, indicative of $\zeta$-$V_4C_{3-x}$. Clear composition discontinuities between $\beta$-$V_2C$ and $\delta$-$VC_{1-x}$ were observed. It can be assumed that at temperatures, where the parallel $\zeta$ phase band is formed, $\zeta$-$V_4C_{3-x}$ is stable, and where the individual $\zeta$ grains are observed, it precipitated upon cooling. At these high temperatures $\zeta$-$V_4C_{3-x}$ could indeed form upon cooling because the carbon diffusivity is 2–3 orders of magnitude higher than at $T \leqslant 1400$°C (a study of carbon diffusivity obtained from layer growth kinetics is in preparation). Thus a decomposition temperature of around 1875°C can be assumed. A modification of the autoclave is in progress in order to confirm these results by means of experiments in which the samples can be quenched from these high temperatures into liquid Sn.

In some V/C diffusion couples spotty areas could be observed within the $\delta$-$VC_{1-x}$ phase band (Fig. 3) which appear blue and orange in polarized light. These areas are probably composed of the ordered phases $V_6C_5$ and/or $V_8C_7$ [31, 32], which is in agreement with the metallographic appearance of hot-pressed and annealed vanadium carbides where the presence of these phases was confirmed by XRD [33].

*3.1.2. The Nb–C system.* The growth rate of $\zeta$-$Nb_4C_{3-x}$ is even lower than that of $\zeta$-$V_4C_{3-x}$. Generally, $\zeta$-$Nb_4C_{3-x}$ could only be observed in $\beta$-$Nb_2C$/C but not in Nb/C diffusion couples and the formation is apparently more influenced by the orientation of the $\beta$-$Nb_2C$ phase. An example of this phenomenon is given in Fig. 4(a) where the $\zeta$ phase did not develop in the form of a phase band but rather in the form of needle-like crystallites which depend on the orientation of $\beta$-$Nb_2C$ grains (indicated by the different color appearance). In favorable cases, however, distinct parallel bands could be observed [Fig. 4(b)] which were well suited for microprobe analysis (see below). Similar orientational effects were recently described for the $\zeta$-$Hf_4N_{3-x}$ phase [34] for which it was shown that a parallel diffusion band does generally not form below 1240°C.

Because of the extremely slow formation of the $\zeta$-$Nb_4C_{3-x}$ phase (e.g. $\geqslant$380 h at 1500°C) and its apparent texture-influenced formation (which gives

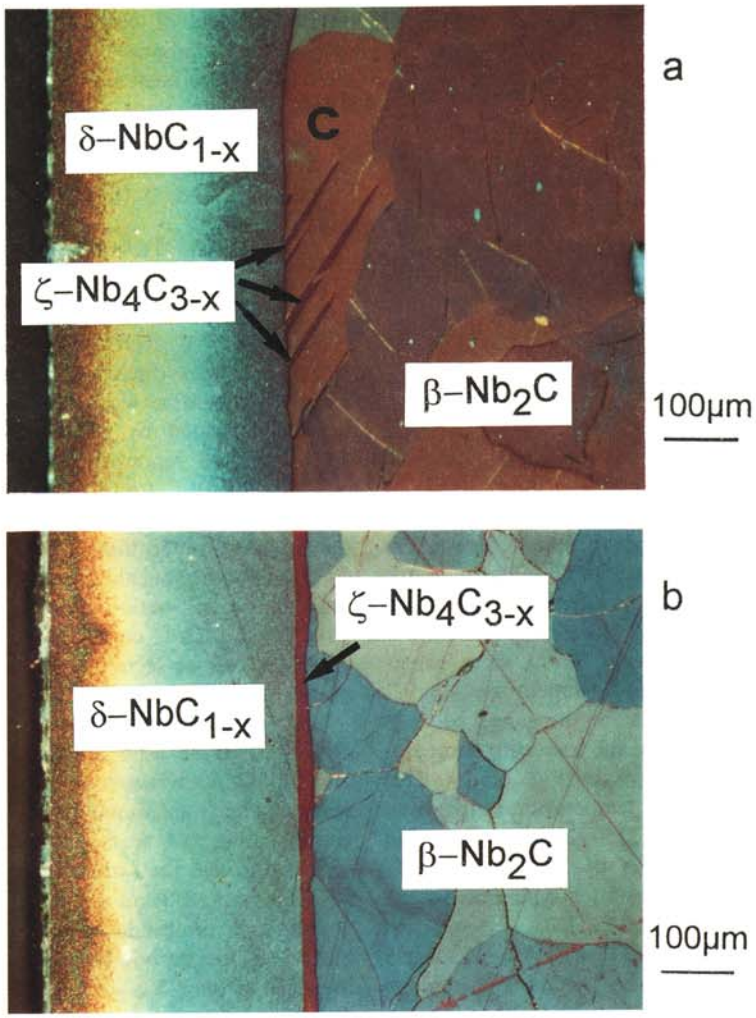


Fig. 4. Microstructures of $\beta$-$Nb_2C$/C diffusion couples annealed at 1500°C for 656 h. Anodically oxidized, polarized light: (a) the formation of $\zeta$-$Nb_4C_{3-x}$ takes place only in certain preferred directions of the $\beta$-$Nb_2C$ phase. Needle-shaped precipitations form from the $\beta/\delta$-interface into the $\beta$-$Nb_2C$ phase in crystallite "C"; (b) in favorable cases a distinct $\zeta$-$Nb_4C_{3-x}$ band forms, accessible for electron microprobe analysis.

rise to some uncertainty as to whether the phase band is absent because of texture effects or because of thermodynamic instability) it was decided to try to determine the decomposition temperature with hot-pressed specimens with compositions of 36–39 at.%C. In a first step, the hot-pressed samples were annealed under argon atmosphere at 1475°C for 340 h. Then the samples were annealed at different temperatures up to 1650°C for 40 h. A powder X-ray diffractogram was taken of each sample. The $\zeta$-$Nb_4C_{3-x}$ phase was present in all four samples at 1547°C (together with $\beta$-$Nb_2C$ and $\delta$-$NbC_{1-x}$, which is the result of the usual inhomogeneity encountered in bulk specimens) and was absent in all four samples after annealing at 1602°C, thus the peritectoid decomposition temperature is to be set at $1575 \pm 27$°C. In the light of the present findings the observations of Brauer and Lesser [10] can be well explained. They had prepared bulk samples at 1800°C and had found weak X-ray reflections of $\zeta$-$Nb_4C_{3-x}$. Despite a prolonged annealing time, they could not increase the amount of this phase obviously because they have annealed their samples above the decomposition temperature. In another study [7] this phase could not be detected as the heat treatments were performed above a temperature of 1600°C.

*3.1.3. The Ta–C system.* In all Ta/C diffusion couples the formation of diffusion bands of $\delta$-$TaC_{1-x}$ and $\beta$-$Ta_2C$ could be easily observed. Figure 5 shows a typical diffusion couple of the system Ta/C. The $\zeta$-$Ta_4C_{3-x}$ phase formed between the $\delta$-$TaC_{1-x}$ and the $\beta$-$Ta_2C$ phase as a rather thin but distinct phase band, the width of which could be increased by applying wedge-type samples. In microsections of such diffusion couples an unambiguous proof of the presence/absence of $\zeta$-$Ta_4C_{3-x}$ was possible with the light optical micro-

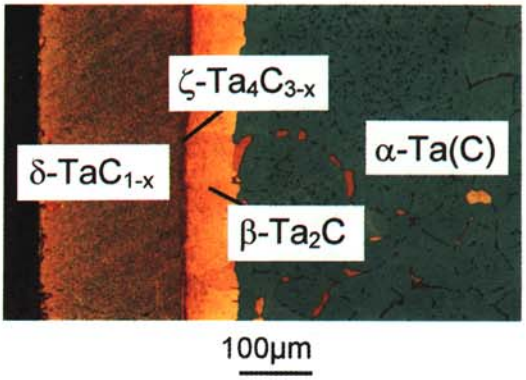


Fig. 5. Microstructure of a Ta/C diffusion couple annealed at 1915 C for 256 h; anodically oxidized, polarized light.

scope. This is shown in Fig. 6(a) (top) where the $\zeta$-$Ta_4C_{3-x}$ phase band can be seen near the tip of the $\beta$-$Ta_2C$ phase band, whereas it is too thin to be observable at a larger sample thickness. Figure 6(b) (bottom) shows a wedge type Ta/C diffusion couple carburized above the decomposition temperature of the $\zeta$-$Ta_4C_{3-x}$ phase. The $\zeta$ phase is absent even at the tip of the $\beta$-$Ta_2C$ phase. From these experiments the decomposition temperature of $\zeta$-$Ta_4C_{3-x}$ was derived to be in the range between 2150 and 2175°C which are the annealing temperatures of the samples shown in Fig. 6(a,b). This value is consistent with the temperature range given by Brizes and Tobin [18] (2150–2250°C). It is also consistent with the findings of Zaplatynsky [17], who observed a Widmannstätten-type microstructure at the carbon-poor side of $\delta$-$TaC_{1-x}$ similar to the appearance shown in Fig. 6(b) in a sample annealed at 2500°C, where the $\zeta$ phase is unstable.

*3.1.4. The Ta–N system.* In samples prepared at a pressure of 2 bar $N_2$ the formation of a thin $\varepsilon$-TaN top layer, followed by a $\beta$-$Ta_2N$ layer, could be observed below 1770°C [Fig. 7(b)]. Under a pressure of 10 bar $N_2$ the decomposition of the $\varepsilon$-TaN phase was found to occur between 1825 ($\varepsilon$-TaN layer present) and 1860°C ($\varepsilon$-TaN layer absent) and at 25 bar $N_2$ between 1873 ($\varepsilon$-TaN layer present) and 1903°C ($\varepsilon$-TaN layer absent). Kieffer *et al.* [24] gave the $\varepsilon$ decomposition temperature of 2000°C at a pressure of 10 bar $N_2$ and Politis and Rejman [25] of 1760°C at more than 100 bar $N_2$.

In samples which were nitrided at pressures of 10 bar $N_2$ or higher, formation of the $\delta$-$TaN_{1-x}$ phase occurred at $T \geqslant 1830$°C and was absent at $T \leqslant 1812°$. The eutectoid decomposition of the $\delta$-$TaN_{1-x}$ into $Ta_2N$ and $\varepsilon$-TaN is in agreement with Gatterer *et al.* [22], who reported this equilibrium to be at $1750 \pm 50$°C.

The cooling rate of the autoclaves was too low to quench $\delta$-$TaN_{1-x}$ and hence a eutectoid decomposition $\delta$-$TaN_{1-x} \rightarrow \varepsilon$-TaN + $\beta$-$Ta_2N$ occurred upon cooling. In Fig. 7(a) the perlitic microstructure caused by this decomposition is shown. In agreement with literature [22, 25] the stability of the $\delta$-$TaN_{1-x}$ phase was found to be very sensitive to small amounts of carbon. The $\delta$-$TaN_{1-x}$ phase band could be almost entirely stabilized if a graphite crucible was heated in the autoclave prior to the nitriding experiments. Both, the presence of the two-phase mixture $\varepsilon$-TaN + $\beta$-$Ta_2N$ in practically carbon-free samples, as well as the presence of the carbon-stabilized $\delta$-$TaN_{1-x}$ were confirmed by XRD.

### 3.2. Homogeneity ranges of phases

*3.2.1. The V-C, Nb-C and Ta-C systems.* In a variety of samples (including different samples prepared at the same temperatures) the phase bands were investigated by microprobe analysis. Figure 8(a,b,c) shows representative EPMA scans across one-half of a V/C (top), a Nb/C (center) and a Ta/C (bottom) diffusion couple. For the V/C couple the $\zeta$ phase was too thin to be detected, for the Nb/C couple the annealing temperature was higher than the decomposition temperature of the $\zeta$ phase. Only for the Ta/C couple some data points for $\zeta$-$Ta_4C_{3-x}$ can be seen. The compositional discontinuities at the phase boundaries are clearly visible.

The compositions of the $\zeta$-$V_4C_{3-x}$ and $\zeta$-$Nb_4C_{3-x}$ phase were measured in V/C, $\beta$-$V_2C$/C and $\beta$-$Nb_2C$/C diffusion couples, two representative scans of which are shown in Fig. 9(a,b). Figure 9(a) shows the EPMA scan in the direction of carbon diffusion across the sample shown in Fig. 1 (at the position marked by an arrow).

Despite a multitude of line scans and measurements near the carbon-rich as well as the metal-rich interface of the $\zeta$-$V_4C_{3-x}$ phase it was not possible to establish the existence of a homogeneity range (according to the achieved precision it is presumably below 0.4 at.%C). All these scans yielded an average composition of 37.9 at.%C (at 1850°C a value of 37.2 at.%C was found which could mean that the composition shifts to a lower carbon content). Ghaneya and Carlson [9] found a maximum amount of $\zeta$-$V_4C_{3-x}$ in an arc-melted sample of a composition of 39.7 at.%C, which was nearly single-phase after homogenization at 1300°C. However, they did not specify whether they had made a carbon analysis or whether they had calculated the composition from the weight of the starting materials (usually a loss of carbon occurs on arc-melting).

In Fig. 9(b) an EPMA scan across one-half of a $Nb_2C$/C diffusion couple is shown where the $\zeta$-$Nb_4C_{3-x}$ phase formed a parallel diffusion band. The discontinuities in the carbon profiles are representative for the two-phase fields $\beta + \zeta$ and $\zeta + \delta$, respectively, and are proof of the stable character of $\zeta$-$Nb_4C_{3-x}$ which was previously in doubt [3]. In contrast to $\zeta$-$V_4C_{3-x}$, a homogeneity range could be measured for the $\zeta$-$Nb_4C_{3-x}$ phase. As determined from three independent scans, agreeing within $\pm 0.1$ at.%C with each other, a range of

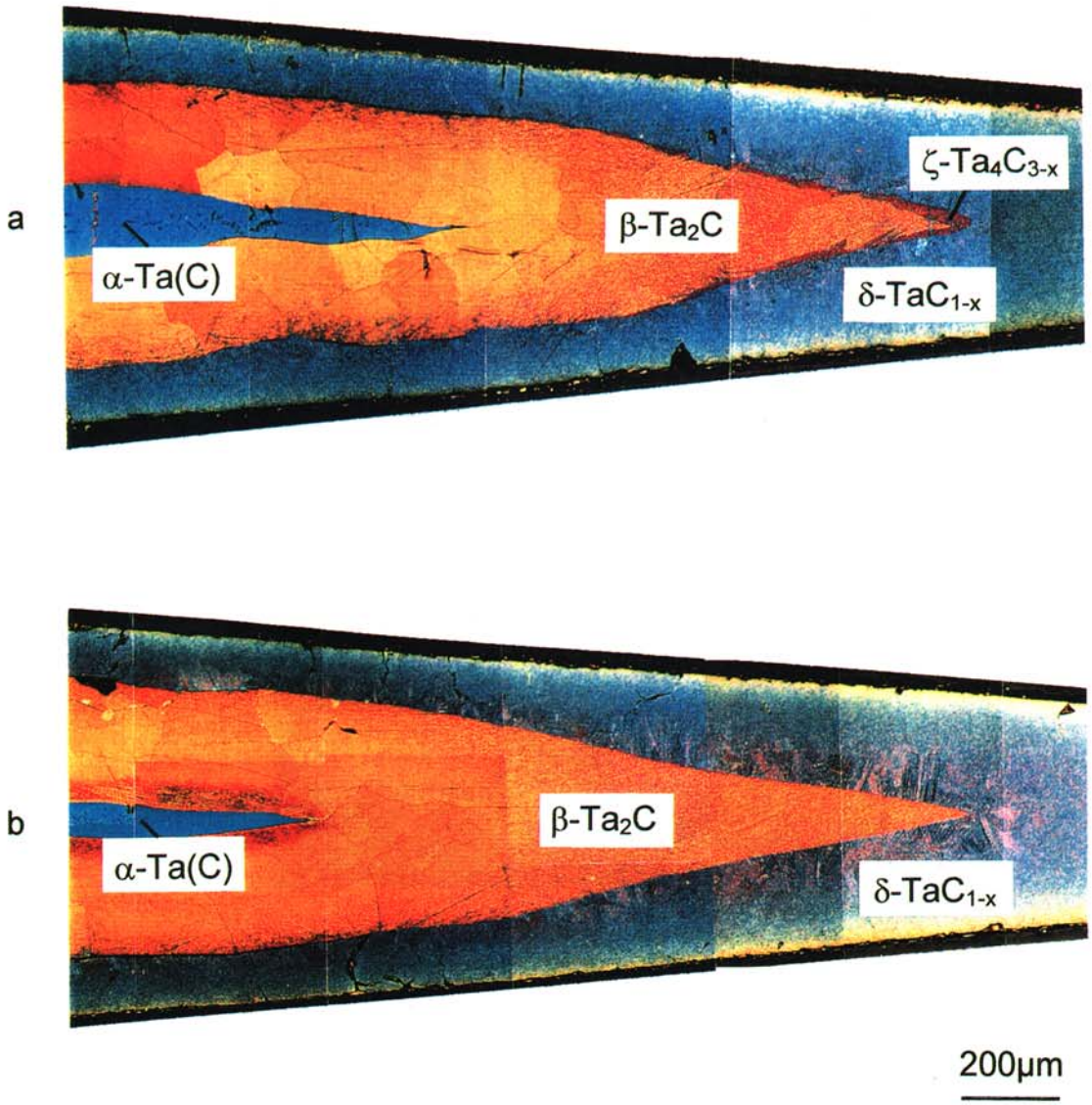


Fig. 6. (a) Microstructure of a wedge-type Ta/C diffusion couple carburized at 2150°C for 8.9 h; anodically oxidized, polarized light. The $\zeta$-$Ta_4C_{3-x}$ phase band can easily be observed but only at the tip of the $\beta$-$Ta_2C$ phase. $\zeta$-$Ta_4C_{3-x}$ is (almost) not visible with light optical microscopy because of its thin band width at larger sample thicknesses; (b) microstructure of a wedge-type Ta/C diffusion couple carburized at 2175°C for 7.2 h; anodically oxidized, polarized light. The $\zeta$-$Ta_4C_{3-x}$ phase did not form, because the sample was annealed above the decomposition temperature of the $\zeta$-$Ta_4C_{3-x}$ phase.

40.1–40.7 at.%C was found. No literature values are available for comparison.

Since the $\zeta$-$Ta_4C_{3-x}$ phase band width in plane sheet diffusion couples is rather small, the composition of the $\zeta$-$Ta_4C_{3-x}$ phase was measured in wedge-type diffusion couples. Accurate microprobe measurements of very heavy elements in combination with light elements are rather difficult [27]. In order to ensure favorable measurement conditions a wedge-type diffusion couple was prepared by annealing a tantalum wedge in a graphite bed for 10 days followed by another annealing step without graphite of another 27 days. This resulted in a $\zeta$ phase band of a lateral extension of more than 100 $\mu$m at the tip of the wedge which allowed a much greater number of EPMA measurement points. Figure 10 shows the microstructure of this diffusion couple and the corresponding carbon profile. From this profile a homogeneity range of 38.2–39.0 at.%C could be measured for the $\zeta$-$Ta_4C_{3-x}$

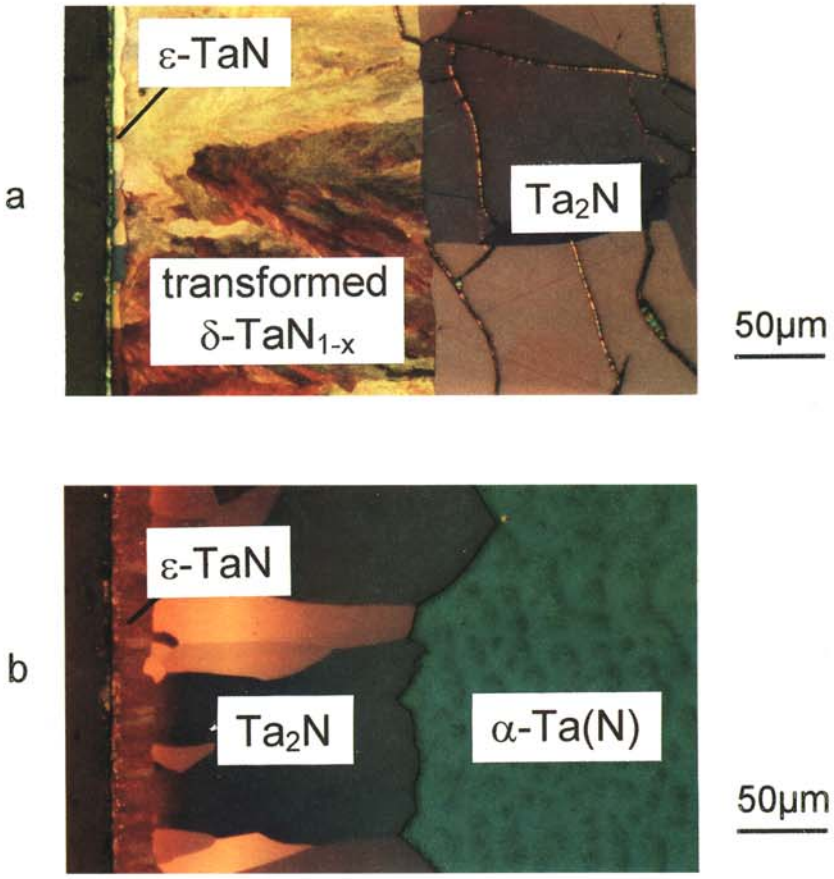


Fig. 7. Microstructures of $Ta/N_2$ diffusion couples; anodically oxidized, polarized light: (a) representative for annealing temperatures $T \geqslant 1830°C$ which is above the temperature of the three-phase equilibrium $\delta\text{-}TaN_{1-x} \rightarrow \beta\text{-}Ta_2N + \varepsilon\text{-}TaN$. The transformation of the $\delta\text{-}TaN_{1-x}$ phase occurred during cooling (perlitic microstructure); (b) representative for annealing temperatures $T \leqslant 1812°C$ and $p(N_2) \geqslant 10$ bar, the $\beta\text{-}Ta_2N$ and $\varepsilon\text{-}TaN$ phases are in equilibrium.

phase (determined from various independent scans) which is lower than the composition of 41.7 at.%C found by Brizes and Tobin [18]. These authors prepared a *ca.* 25$\mu$m thick $\zeta\text{-}Ta_4C_{3-x}$ phase band by a carburizing/decarburizing procedure on apparently thick diffusion couples. Presumably, they could not perform a direct microprobe carbon analysis and derived the carbon content from the Ta content. Also different anticontamination techniques could account for diverging results. Our own measurements showed that without the use of a cold trap and an oxygen jet, that the carbon contamination caused a virtual increase of the carbon content of about 3 at.%C.

In Fig. 11(a,b,c) the results of the EPMA measurements for the three carbide systems are graphically summarized. The values for the carbon contents in the metals were taken from published data [15]. The phase boundaries found for the $\beta\text{-}Me_2C$ phases disagree somewhat with the literature. Generally, the upper compositional limit of $\beta\text{-}Me_2C$ was found to be more carbon-rich than compiled data [15]. For $\beta\text{-}V_2C$ a search in the original literature shows the carbon-rich phase boundary to be located between 35 at.%C [8] and 37 at.%C [35] so that the present findings are within this range. In an extensive report on microprobe analysis of carbides by Bastin and Heijligers [36] an EPMA scan is shown which indicates a similar value as observed in the present study. The homogeneity range of the $\beta\text{-}Nb_2C$ phase is 2 at.%C in the investigated temperature range and hence does not even include the composition "$Nb_2C$" (i.e. 33.3 at.%C).

Also the compositions measured for the phase boundaries of the $\beta\text{-}Ta_2C$ phase were found to be richer in carbon than previously assumed in the

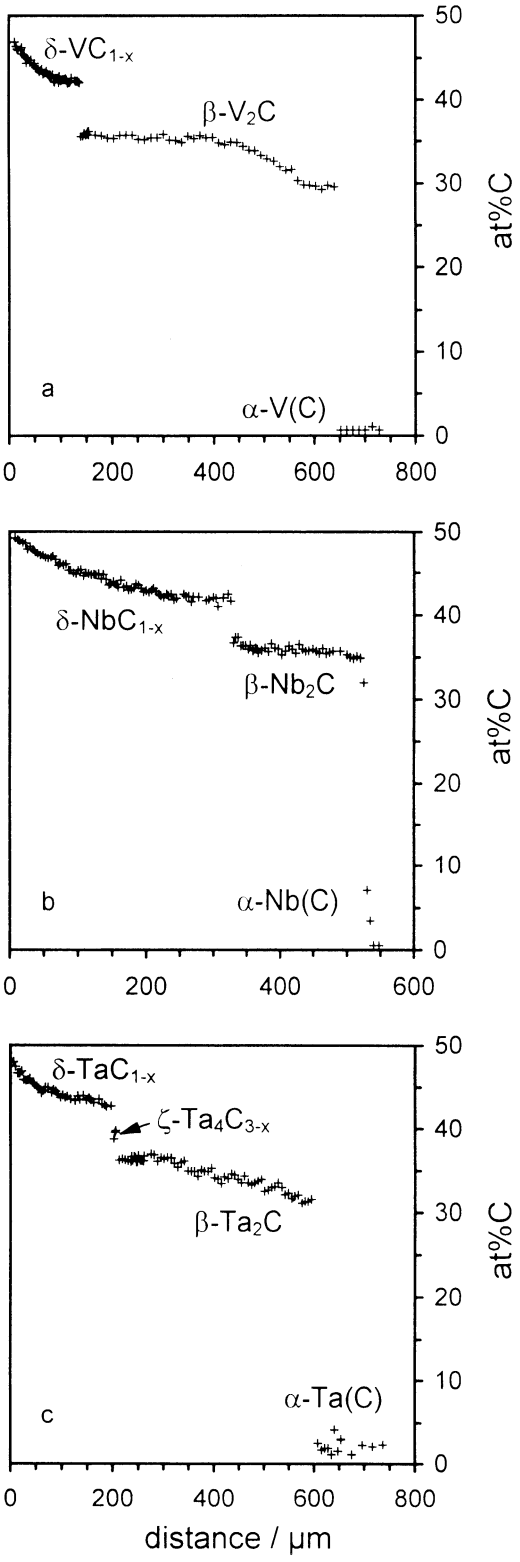


Fig. 8. (a) EPMA scan across the phases of a V/C diffusion couple in the direction of the carbon diffusion. The $\zeta$-$V_4C_{3-x}$ phase was too thin to be detected. (b) EPMA scan across the phases of a Nb/C diffusion couple in the direction of the carbon diffusion. The sample was annealed above the decomposition temperature of $\zeta$-$Nb_4C_{3-x}$. (c) EPMA scan across the phases of a Ta/C diffusion couple in the direction of the carbon diffusion. The sample was annealed below the decomposition temperature of $\zeta$-$Ta_4C_{3-x}$ but only a few data points for the latter could be recorded.

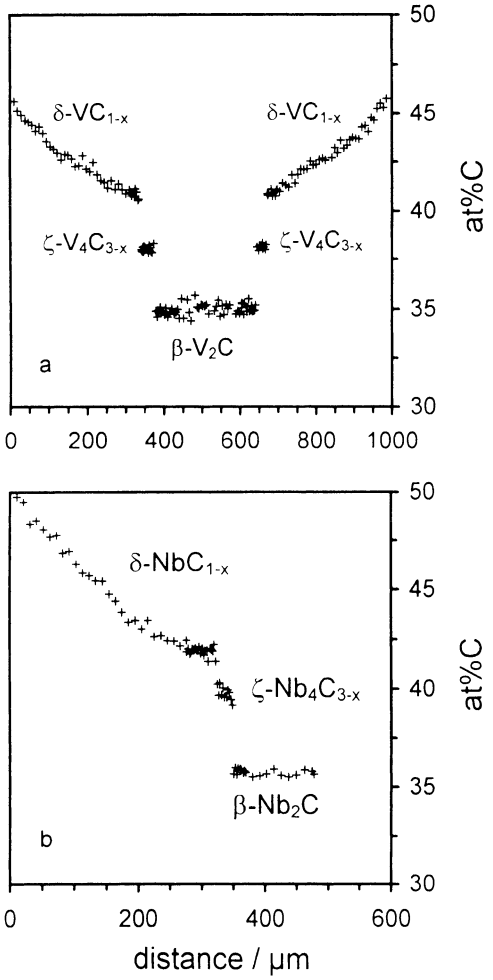


Fig. 9. (a) EMPA scan across the $\beta$-$V_2C$/C diffusion couple shown in Fig. 1 (position marked with arrow) where the $\zeta$ phase had formed. The homogeneity region of the $\zeta$-$V_4C_{3-x}$ phase is very small. (b) EPMA scan across a $\beta$-$Nb_2C$/C diffusion couple including a $\zeta$-$Nb_4C_{3-x}$ phase band. A homogeneity region of 40.1–40.7 at.%C could be measured (from three line scans).

ASM Handbook [15]. Below 1900 °C the homogeneity range of $\beta$-$Ta_2C$ is only 1.5 at.%C; above 1900 °C it widens.

The compositional discrepancies encountered for the $\beta$-$Me_2C$ phases could be due to the uncertainty of measuring the location of phase boundaries by the usual combination of metallography, XRD and gross-chemical analysis of bulk specimens. The carbon-poor boundary for all $\delta$-$MeC_{1-x}$ phases was

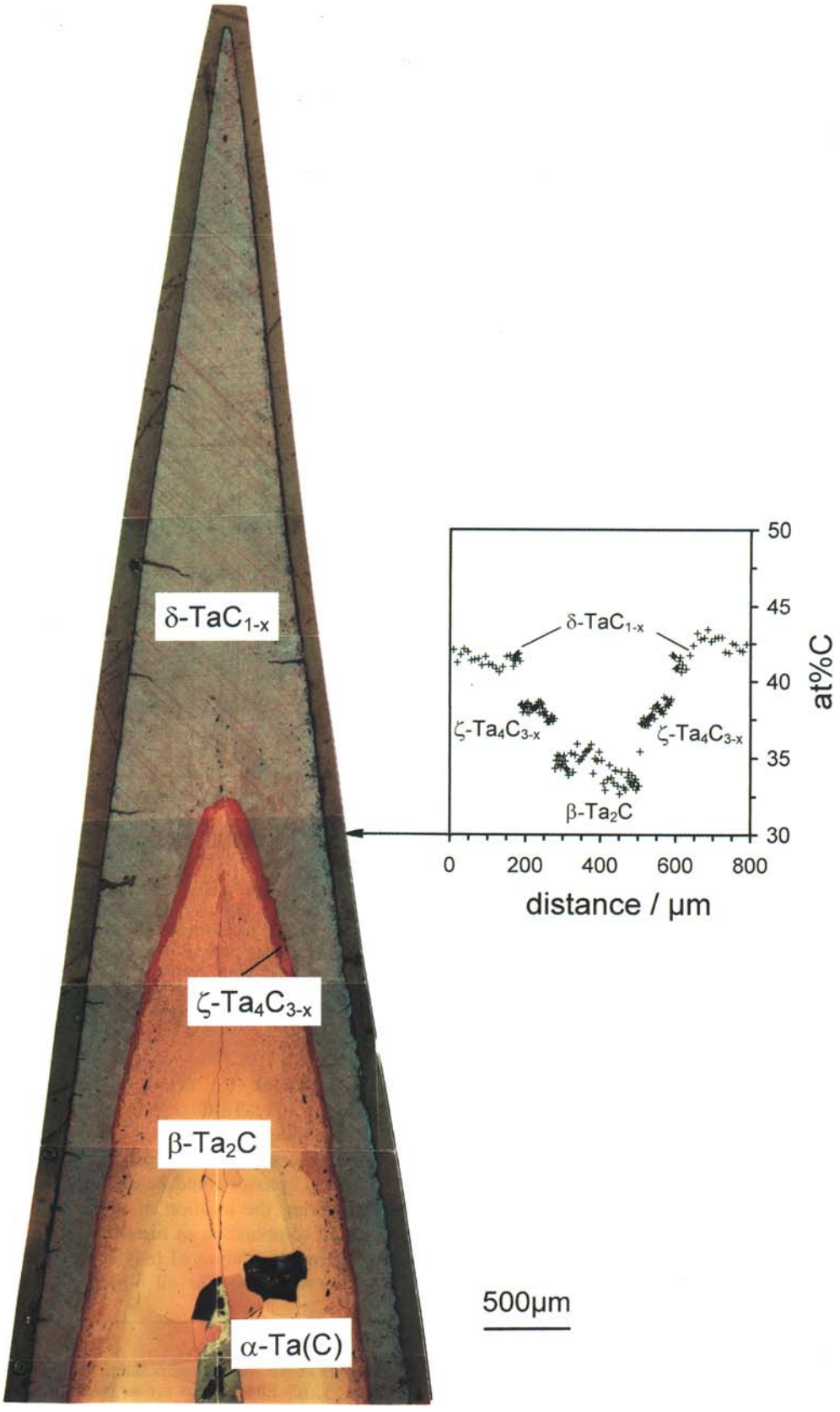


Fig. 10. Left: Microstructure of a wedge-type Ta/C diffusion couple annealed at 1900°C for 256 h and re-annealed without graphite at 1900°C for 650 h; anodically oxidized, polarized light. The $\zeta$-$Ta_4C_{3-x}$ phase band is enlarged at the tip of the $\beta$-$Ta_2C$ phase where $\beta$-$Ta_2C$ is carbon saturated; right: EPMA scan across the position marked with an arrow from which the homogeneity region of $\zeta$-$Ta_4C_{3-x}$ could be established.

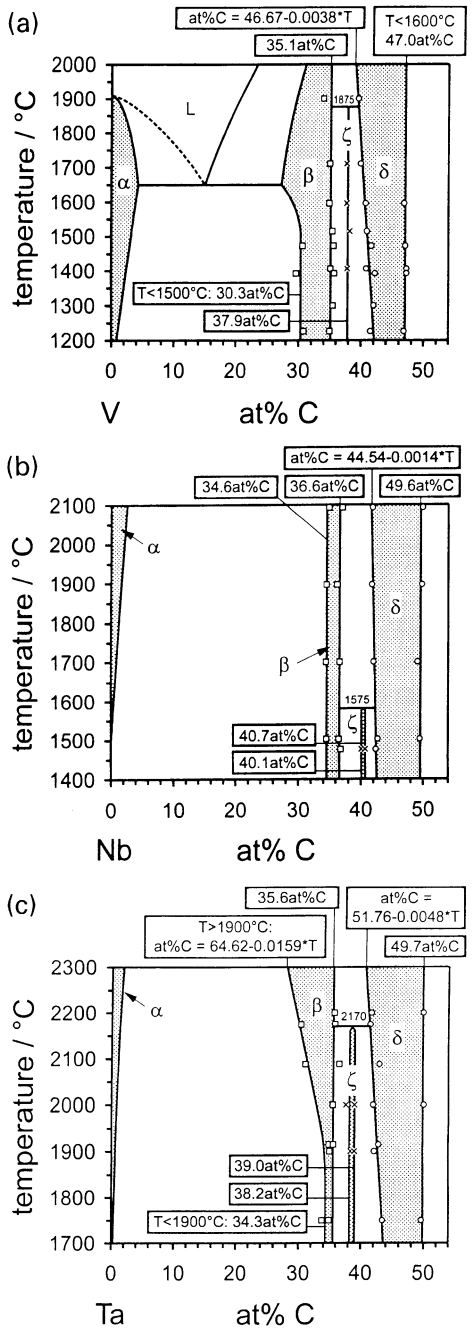


Fig. 11. Summarized results of the EPMA measurements for the homogeneity regions of the phases in the V–C (a), Nb–C (b) and Ta-C (c) systems. Temperatures in the equations are given in °C, the values of the carbon solubility in the α phase is taken from the literature [15].

found to be dependent on temperature (the higher the temperature the lower the carbon concentration), whereas the carbon-rich boundaries were found to be independent of temperature. Because of the restricted lateral resolution of the EPMA measurements and the steeply rising carbon concentration profile near the sample surface the carbon-rich compositions of the $\delta$-$MeC_{1-x}$ phases were not taken from the concentration profile. Instead the outermost tip of the wedge was used which is homogeneous and identical with the surface composition in equilibrium with graphite [27]. A linear dependency as a function of temperature was found to fit the phase boundaries of these phases. The carbon-poor limit of the homogeneity range of $\delta$-$VC_{1-x}$ and $\delta$-$NbC_{1-x}$ is in good, and the carbon-rich composition in excellent, agreement with the ASM compilation (although the NbC boundaries are drawn with a broken line there).

The carbon-poor boundary of the $\delta$-$TaC_{1-x}$ phase was found to be temperature dependent. At the upper temperature limit of the present investigation this phase was found to be more carbon deficient than given in the literature [15], whereas at the lower limit agreement was found. The carbon-rich boundary of $\delta$-$TaC_{1-x}$ was found to be constant, which is in good agreement with previous data.

*3.2.2. The Ta–N system.* Figure 12 shows a typical $Ta/N_2$ wedge-type diffusion couple for $T = 1873$°C, $p(N_2) = 25.1$ bar, $t = 20.5$ h. Away from the tip of the wedge, where the α-Ta(N) core is still present, the phase bands of ε-TaN and $\delta$-$TaN_{1-x}$ are rather thin. Towards the tip of the wedge, where the α-Ta(N) core disappears, the width of the $\delta$-$TaN_{1-x}$ phase band increases. At the tip, where the β-$Ta_2N$ phase is no longer present the width of the ε-TaN phase band also widens substantially. Thus, as indicated by Fig. 12, the EPMA scans had to be made at different locations (A,B,C) in order to measure the homogeneity ranges of all the phases present at the annealing temperature.

Because of the extremely fine-lamellar microstructure and the limited spatial resolution of the EPMA the diffusion profiles in the transformed $\delta$-$TaN_{1-x}$ phase band did not show significant scatter. Therefore, with negligible nitrogen diffusion upon cooling the EPMA profile is identical to the diffusion profile in non-transformed $\delta$-$TaN_{1-x}$ allowing the measurement of the homogeneity range of $\delta$-$TaN_{1-x}$. The results of all EMPA measurements are graphically summarized in Fig. 13. The eutectoid composition of $\delta$-$TaN_{1-x}$ is located at 43.4 at.%N ($TaN_{0.77}$) and is in fair agreement with Gatterer *et al.* [22] who estimated 42 at.%N. The solubility of nitrogen in tantalum shows a linear dependence on temperature and increases from 6.1 at.%N at 1500°C to 9.5 at.% at 1940°C, also in good agreement with the data of previous studies [19, 20]. The homogeneity region of the β-$Ta_2N$ phase widens with increasing temperature. Above a temperature of 1700°C the nitrogen-rich phase boundary remains constant and is located at 33.5 at.%N, near the stoichiometric composition.

A variety of line scans across the tip of wedge-type diffusion couples showed that the homogeneity

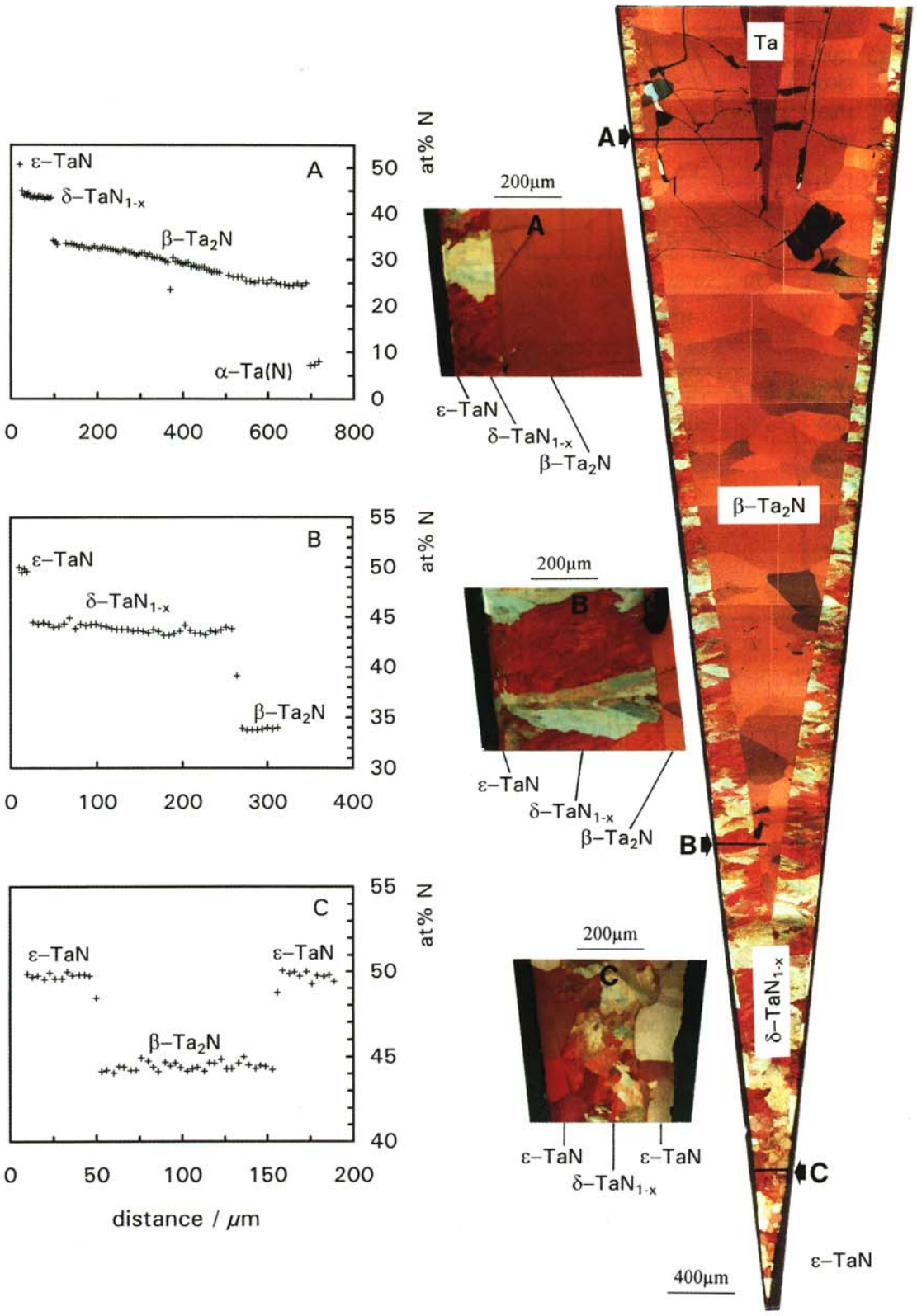


Fig. 12. Microstructure of a wedge type $Ta/N_2$ diffusion sample prepared at 1873°C/25 bar$N_2$, $t$ = 20.5 h; polarized light. EPMA scans were performed at different positions, where the different phase bands showed sufficient lateral extensions. Some examples of line scans of measuring the homogeneity ranges of the various phases are given (locations A, B and C). Note the enlargement of phase bands upon decreasing sample thickness.

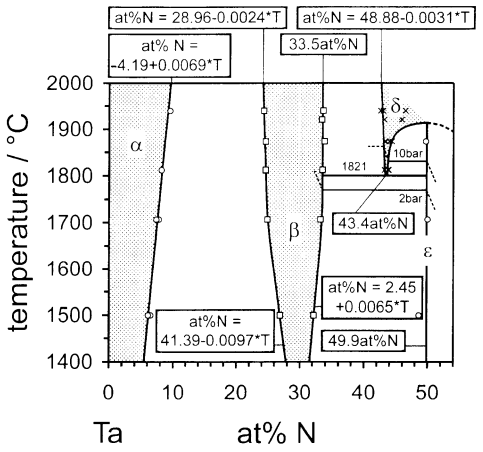


Fig. 13. Summarized results of the EPMA measurements for the homogeneity regions of the phases in the Ta–N system. The temperatures in the equations are given in °C.

range of $\varepsilon$-TaN is below 0.4 at.%N. This value was derived from statistical considerations [27].

The phase boundaries of the various nitride phases are in good agreement with the compilation in the ASM handbook [15], which in turn is based on the phase diagram proposed by Gatterer *et al.* [22].

## 4. CONCLUSION

The arrangement of phases in the form of spatially resolved parallel phase bands that is achieved in multiphase diffusion couples is a powerful tool to characterize systems with respect to phase stabilities and composition of phase boundaries.

Portions of phase diagrams of the V–C, Nb–C, Ta–C and Ta–N systems were reinvestigated and the results are thought to be much less influenced by uncertainties usually encountered with the examination of bulk samples. The $\zeta$-$Me_4C_{3-x}$ phases were characterized in detail, i.e. the composition of the $\zeta$-$V_4C_{3-x}$ phase could be established and the discrepancies in the literature with respect to thermal stability could be explained. For the $\zeta$-$Nb_4C_{3-x}$, $\zeta$-$Ta_4C_{3-x}$, $\delta$-$TaN_{1-x}$ and $\varepsilon$-TaN phases the homogeneity range and decomposition temperatures could be established. For investigating the stability of $\zeta$-$Nb_4C_{3-x}$ the diffusion couple technique is somewhat less powerful because the parallel layer formation is sometimes absent which is usually the case when phases are formed from cooling or at comparatively low temperatures (e.g. $T < 1240$ °C in the Hf–N system).

As a suggestion for further work $\beta$-$Me_2C$/C diffusion couples should be applied which would allow to measure the $Me_2C$–MeC phase equilibria at high temperatures.

*Acknowledgements*—The help of Dr J. Bauer, Member of CNRS at the University of Rennes I, Rennes, France and Mr M. Bohn, Member of CNRS at the IFREMER Brest, France, with the microprobe measurements is gratefully acknowledged. This work was financially supported by the Austrian National Science Foundation FWF, Project No. 8784 and by the Austrian Academy of Sciences, project No. PICS-134 within a France–Austria cooperation. For the latter the help of Mrs Mag. Irene Häupler is particularly acknowledged.

## REFERENCES

1. Carlson, O. N., Ghaneya, A. H. and Smith, J. F., in *Phase Diagrams of Binary Vanadium Alloys*. ASM International, Metals Park, OH, 1989.
2. Huang, W., *Z. Metallk.*, 1991, **82**, 174.
3. Smith, J. F., Carlson, O. N. and DeAvillez, R. R., *J. nucl. Mater.*, 1987, **148**, 1.
4. Frisk, K. and Fernández, Guillermet A., *J. Alloys Comp.*, 1996, **238**, 167.
5. Storms, E. K. and McNeal, R. J., *J. Phys. Chem.*, 1962, **66**, 1401.
6. Storms, E. K., Lowe, A., Baca, E. and Griffin, J., *High Temp. Sci.*, 1973, **5**, 276.
7. Rudy, E., Windisch, S. and Brukl, C. E., *Planseeber. Pulvermet.*, 1968, **16**, 3.
8. Khaenko, B. V. and Fak, V. G., *Inorg. Mater.*, 1978, **14**, 1011.
9. Ghaneya, A. H. and Carlson, O. N., *J. less-common Metals*, 1985, **109**, 57.
10. Brauer, G. and Lesser, R., *Z. Metallk.*, 1959, **50**, 8.
11. Storms, E. K. and Krikorian, N. H., *J. Phys. Chem.*, 1960, **64**, 1471.
12. Elliot, E., *Trans. Am. Soc. Metals*, 1961, **53**, 13.
13. Yvon, K. and Parthé, E., *Acta crystallogr. B*, 1970, **265**, 149.
14. Storms, E. K., in *Phase Relationships and Electrical Properties of Refractory Carbides and Nitrides*, Vol. 10, ed. L. Roberts. Solid State Chemistry, Butterworth, London, 1972, p. 37.
15. Handbook of Binary Alloy Phase Diagrams, ed. T. B. Massalski. ASM International, Metals Park, OH, 1990.
16. Lesser, R. and Brauer, G., *Z. Metallk.*, 1958, **49**, 622.
17. Zaplatynsky, I., *J. Am. Ceram. Soc.*, 1966, **49**, 109.
18. Brizes, W. F. and Tobin, J. M., *J. Am. Ceram. Soc.*, 1967, **50**, 115.
19. Fromm, E., *J. less-common Metals*, 1968, **14**, 113.
20. Gebhardt, E., Seghezzi, H. and Fromm, E., *Z. Metallk.*, 1961, **52**, 464.
21. Booker, P. H. and Bruki, C. E., AFML-TR-69-117, Part VI.
22. Gatterer, J., Dufek, G., Ettmayer, P. and Kieffer, R., *Monatsh. Chem.*, 1975, **106**, 1137.
23. Brauer, G. and Zapp, K. H., *Z. Anorg. Allg. Chem.*, 1954, **277**, 1.
24. Kieffer, R., Ettmayer, P., Freudhofmeier, M. and Gatterer, J., *Monatsh. Chem.*, 1971, **102**, 483.
25. Politis, C. and Rejman, G., Report No.KfK- Ext.6/78-1. Kernforschungzentrum Karlsruhe, Germany, 1978.
26. Lengauer, W., Bauer, J., Guillou, A., Ansel, D., Bars, J-P., Bohn, M., Etchessahar, E., Debuigne, J. and Ettmayer, P., *Mikrochim. Acta*, 1992, **107**, 303.
27. Lengauer, W., Bauer, J., Bohn, M., Wiesenberger, H. and Ettmayer, P., *Mikrochim. Acta*, 1997, **126**, 279.
28. Lengauer, W., Rafaja, D., Täubler, R., Kral, C. and Ettmayer, P., *Acta metall. mater.*, 1993, **12**, 3505.
29. Rafaja, D., Lengauer, W. and Ettmayer, P., *Acta mater.*, 1996, **44**, 4835.
30. Lengauer, W. and Ettmayer, P., *J. Phase Equil.*, 1993, **14**, 162.

31. Billingham, J., Bell, P. S. and Lewis, M. H., *Phil. Mag.*, 1972, **25**, 602.
32. Alyamovskii, S. I., Gel'd, P. V., Shveikin, G. P. and Shchetnikov, E. N., *Russ. J. Inorg. Chem.*, 1968, **13**, 472.
33. Lipatnikov, V., Lengauer, W., Ettmayer, P., Keil, E., Groboth, G. and Kny, E., *J. Alloys Comp*, 1997, **261**, 192.
34. Lengauer, W., Rafaja, D., Zehetner, G. and Ettmayer, P., *Acta mater.*, 1996, **44**, 3331.
35. Storms, E. K., in *The Refractory Carbides*. Academic Press, New York, 1973.
36. Bastin, G. F. and Heijligers, H. J. M., in *Quantitative Electron Probe Microanalysis of Carbon in Binary Carbides*. University of Technology Eindhoven, 1990.